

Prediction of high-frequency intrinsic localized modes in Ni and Nb

M. Haas,¹ V. Hizhnyakov,¹ A. Shelkan,¹ M. Klopov,² and A. J. Sievers³

¹*Institute of Physics, University of Tartu, Riia 142, EE-51014 Tartu, Estonia*

²*Institute of Physics, Tallinn University of Technology, Ehitajate 5, EE-19086 Tallinn, Estonia*

³*Laboratory of Atomic and Solid State Physics, Cornell University, Ithaca, New York 14853, USA*

(Received 21 March 2011; revised manuscript received 29 August 2011; published 13 October 2011)

It is found that in some metals, an intrinsic localized mode may exist with frequency above the top of the phonon spectrum. The necessary condition, requiring a sufficiently high ratio of quartic to cubic anharmonicity, may be fulfilled because of screening of the interaction between ions by free electrons. Starting from the known literature values of the pair potentials, we have found that in Ni and Nb the derived localized mode condition is fulfilled. Molecular-dynamics simulations of the nonlinear dynamics of Ni and Nb confirmed that high-frequency intrinsic localized modes may exist in these metals.

DOI: [10.1103/PhysRevB.84.144303](https://doi.org/10.1103/PhysRevB.84.144303)

PACS number(s): 63.20.Pw, 05.45.Yv, 63.20.Ry

I. INTRODUCTION

The study of vibrational energy localization in highly excited small molecules is well known, and a number of reviews have appeared.^{1–4} The idea of localization in perfect anharmonic lattices was considered by Kosevich and Kovalev⁵ for the case of a monatomic chain with nearest-neighbor harmonic, cubic, and quartic anharmonic interactions. They showed that an envelope solitonlike excitation with frequency above the top of the phonon band could exist for sufficiently weak cubic interactions. Somewhat later, strongly localized vibrational modes in anharmonic lattices were proposed in Refs. 6 and 7. The realization that this new excitation phenomenon only required nonlinearity plus discreteness expanded the topic in different directions, ranging from analytical considerations^{6–9} to molecular-dynamics (MD) simulations.^{10–12} The early reviews of the resulting field focused on predicting different processes.^{13–15} These excitations, which are often referred to as intrinsic localized modes (ILM's), discrete breathers, or discrete solitons, have now been identified in different driven physical systems, including electronic and magnetic solids, Josephson junctions, micromechanical arrays, optical waveguide arrays, and laser-induced photonic crystals.^{16–18}

In numerical studies of ILM's in atomic lattices, different two-body potential models such as Lennard-Jones, Born-Mayer-Coulomb, Toda, and Morse potentials as well as their combinations have been used in the past. All of these potentials show strong softening with increasing vibrational amplitude, and the ILM's found in these simulations always drop down from the optical band(s) into the phonon gap, if there is one. (See Refs. 19–22, where ILM's in alkali halide crystals have been calculated.) Consequently, it has been assumed that the softening of atomic bonds with increasing vibrational amplitude is a general property of crystals, and therefore ILM's with frequencies above the top phonon frequency cannot occur. However, a recent inelastic neutron-scattering investigation of the vibrational excitations in uranium (α -U) in thermal equilibrium showed some degree of localization near the top of the phonon spectrum at elevated temperatures.²³ For this to occur, the pair potentials in this metal must be fundamentally different from those describing alkali halide crystals. Because the electrons at the Fermi surface provide

an essential contribution to the screening of the ion-ion interaction in metals, there is no *a priori* reason to expect the anharmonicities of these two very different systems to be similar.

The purpose of this paper is to explore the ILM properties in nickel and niobium by starting from the embedded-atom model (EAM). This technique allows one to find the potential energy of vibrations in metals, taking the screening effects into account.^{24,25} Our findings show that ILM's may be expected to occur in both of these metallic crystals. In the next section, we illustrate how the elastic springs of the atomic bonds are to be renormalized to give the minimal condition for localized mode production. In the small ILM amplitude limit, two additive contributions to the renormalization are identified: the positive one given by the quartic anharmonicity and the negative one determined by the square of cubic anharmonicity. The ILM appears above the phonon spectrum when the first contribution exceeds the second one. For the monatomic chain with nearest-neighbor interactions, this condition agrees with that found by Kosevich and Kovalev⁵ and it corresponds to a rather high ratio of quartic to cubic anharmonicities, but in three-dimensional (3D) lattices a smaller ratio is required. Our calculations demonstrate that in Ni and Nb this ILM condition is fulfilled. The molecular-dynamics simulations for nickel and for niobium confirming this result are described in Sec. III followed by some conclusions in Sec. IV.

II. THRESHOLD CONDITION FOR ILM

One can readily present an argument in favor of the localized mode possibility in metals. The point is that the essential contribution to the screening of the atomic interactions in metals comes from free electrons at the Fermi surface. Due to their well-defined energy and the oscillating character of the wave functions of these electrons (Friedel oscillations), the resulting pair potentials may acquire a nonmonotonic or even oscillatory dependence on the atomic distance.²⁶ One consequence is that the ion-ion attractive force, at intermediate distances, may be enhanced resulting in an amplification of even anharmonicities for the resulting two-body potentials. This effect can counteract the underlying softening associated with the bare potentials with a moderate increase of vibrational

amplitudes to permit the existence of ILM's above the top of the phonon spectrum.

Let the anharmonic potential describing the nearest-neighbor interactions for a 1D monatomic chain be represented by

$$U = \sum_n \sum_{p=2}^4 \frac{K_p}{p} (u_{n+1} - u_n)^p, \quad (1)$$

where K_2 is the harmonic force constant and K_3, K_4 are the anharmonic ones, and u_n is the displacement of the n th atom from its equilibrium position. The condition for the formation of an ILM with the frequency above the top of the phonon spectrum, given in Ref. 5, is $\kappa = 3K_2K_4/4K_3^2 > 1$.

To obtain the minimal condition more generally, we use the equation for renormalization of the elastic springs of the atomic bonds by the ILM derived in Refs. 27 and 28, which is

$$\delta K_{2n} = 2(\sin^2(\omega_L t) \partial^2 V^{\text{anh}} / \partial r_n^2), \quad (2)$$

where δK_{2n} is the change produced in the harmonic spring of the pair potential of bond number n . Here ω_L is the frequency of ILM, V^{anh} is the anharmonic part of the potential, the second derivative is taken for the distance of the bond $r_n = r_{0n} + \bar{A}_n \cos(\omega_L t) + \bar{\xi}_n$, where r_{0n} is the length of the bond, \bar{A}_n is the amplitude of vibration of this bond,

$$\bar{\xi}_n = \sum_{n_l} \bar{g}_{nn_l} \langle \partial V^{\text{anh}} / \partial r_{n_l} \rangle \quad (3)$$

is the dc change (usually extension) of its length due to the ILM, $\bar{g}_{nn_l} = g_{nn_l} - g_{n'n_l} - g_{nn_l'} + g_{n'n_l'}$, n and n' are the indexes of two ends of the bond n , $g_{nn_l} = -(M_n M_{n_l})^{-1/2} \sum_i e_{ni} e_{n_l i} \omega_i^{-2}$ is the static limit of the lattice Green's function, e_{ni} is the polarization vector of the phonon i for the bond n , ω_i is the frequency of the phonon, and M_n is the mass of the atom n .

For a small amplitude ILM, one need only consider cubic and quartic anharmonicity. In this approximation, Eqs. (2) and (3) take the form

$$\delta K_{2n} = 2K_3 \bar{\xi}_n + \frac{3}{4} K_4 \bar{A}_n^2, \quad (4)$$

$$\bar{\xi}_n = \frac{1}{2} \sum_{n_l} \bar{g}_{nn_l} K_{3n_l} \bar{A}_{n_l}^2. \quad (5)$$

Usually the first term in Eq. (4) is negative while the second term is positive. The bond will harden with increasing amplitude of vibrations, and an ILM will shift up from the phonon band if the absolute value of the first term is smaller than the second term. To fulfill this condition, the value of the parameter κ needs to be sufficiently large. This value depends not only on the pair potentials but also on the type and dimension of the lattice.

We consider first δK_2 in a monatomic chain with nearest-neighbor interactions. In this case, $n' = n + 1$ and g_{nn_l} depends on $|n - n_l|$. Therefore, $\bar{g}_{nn_l} = 2g_{nn_l} - g_{n+1n_l} - g_{n-1n_l}$. From the equations of motion, one gets $\omega_i^2 e_{in} = (K_2/M)(2e_{in} - e_{in+1} - e_{in-1})$. Multiplying both sides of this equation by $\omega_i^{-2} e_{in_l}$ and summing up over i , we get $\delta_{nn_l} = -K_2 \bar{g}_{nn_l}$. Consequently, the dc lattice expansion equals

$$\bar{\xi} = -(K_3/2K_2) \bar{A}^2 \quad (6)$$

(index n is now omitted). Therefore,

$$\delta K_2 = (3K_4/4 - K_3^2/K_2) \bar{A}^2. \quad (7)$$

The bond will harden with increasing amplitude of vibrations and an ILM will shift up from the phonon band if $\kappa = 3K_2K_4/4K_3^2 > 1$. This condition is identical to that found in Ref. 5 for localized vibrations in the chain. A detailed discussion of this condition has also been given in Ref. 29. [For arbitrary amplitude, the ILM condition for the potential described by Eq. (1) is also given in Ref. 30.]

Let us apply now Eqs. (4) and (5) to 3D lattices. We treat an even symmetry ILM in a monatomic fcc or bcc lattice with the main motion directed along the shortest bond. Note that the high-energy edge of the phonon DOS in both of these lattices corresponds to the short-wavelength phonons. Therefore, the initial ILM under consideration, shifting up from the phonon band, resembles a wave packet of the standing longitudinal plane waves; it has a large spatial extent.

We assume that the anharmonic interactions are well localized. This allows one to include in Eq. (5) only contributions of the shortest bonds in the xy direction (fcc lattice) or in the xyz direction (bcc lattice). The factors \bar{g}_{nn_l} in this equation tend to zero with increasing $|n - n_l|$. Therefore, if the ILM is close to the threshold limit, then the corresponding amplitudes of vibrations of all these bonds at the contributing n_l sites in Eq. (5) are almost the same, and so the dc distortion

$$\bar{\xi} \simeq -\frac{2K_3 \bar{A}^2}{MN} \sum_q \sum_{n=0}^{N-1} \frac{1 - \cos(qr_0)}{\omega_q^2} e^{iqr_0(n-N/2)}, \quad (8)$$

where Nr_0 is the distance between the border atoms in the direction of the main vibration (r_0 is the equilibrium first-neighbor distance), ω_q is the frequency of the longitudinal waves, and q is the wave number acquiring the discrete values $q = \pi k/r_0 N$ with $k = -N/2, -N/2 + 1, \dots, N/2 - 1$ (N is even). In the $N \rightarrow \infty$ limit, only the term $k = 0$ contributes, so

$$\bar{\xi} = -(K_3/2\bar{K}_2) \bar{A}^2, \quad (9)$$

where $\bar{K}_2 = Mv_l^2/r_0^2$ is the mean elastic spring in the bulk and v_l is the longitudinal velocity of sound. Comparing this equation for $\bar{\xi}$ with Eq. (6) and considering that \bar{K}_2 is larger than K_2 , we conclude that the expansion by an ILM in a 3D lattice is hindered as compared to the chain, a physically intuitive result. Inserting Eq. (9) for $\bar{\xi}$ into Eq. (4), we get δK_2 . The hardening of the bonds in 3D lattices takes place and an ILM shifts up from the phonon band if

$$\tilde{\kappa} = 3\bar{K}_2 K_4/4K_3^2 > 1. \quad (10)$$

This condition is easier to fulfill than the 1D condition for $\kappa > 1$.

III. MD SIMULATIONS

A. ILM's in nickel

The potential energy of Ni developed in Ref. 31 has the customary form for the embedded atom model,^{24,25}

$$E_{\text{tot}} = \frac{1}{2} \sum_{nn'} V(r_{nn'}) + \sum_n F_n(\bar{\rho}_n), \quad (11)$$

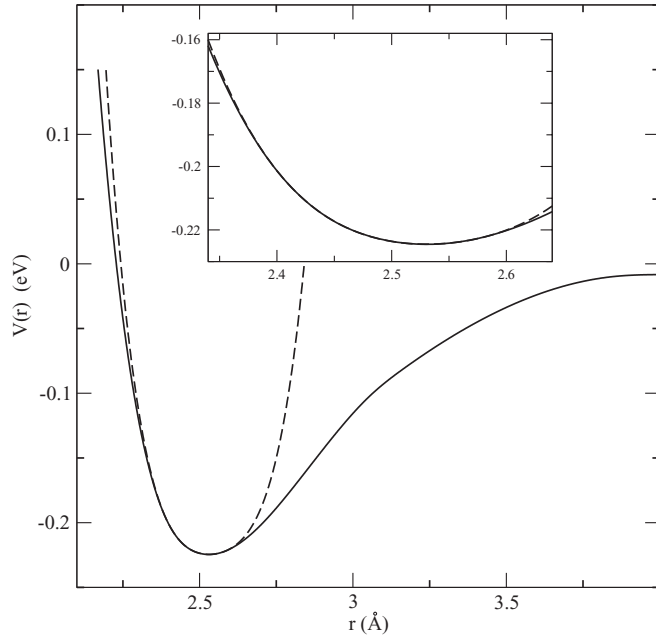


FIG. 1. The pair potential $V(r)$ of Ni (solid line) and its approximation by the fourth-order polynomial (dashed line). The inset shows an expanded view.

where $V(r_{nn'})$ is a pair potential as a function of the distance $r_{nn'}$ between atoms n and n' , F_n is the embedding energy of atom n as a function of the electron density $\bar{\rho}_n = \sum_{n' \neq n} \rho(r_{nn'})$ induced at atom n by all other atoms in the system, and $\rho(r_{nn'})$ is the electron density at atom n due to atom n' as a function of the distance between them. The second term in Eq. (11) is volume-dependent. Its contribution is essential for determining the equilibrium configuration of the lattice. Below we use the effective pair format in which this term has only quadratic and higher-order contributions with respect to the displacement of atoms from their equilibrium position in the lattice. For small displacements compared to the lattice constant, this term is usually small. In Ni, the corresponding correction of the elastic springs is of the order of 1%, and the correction of the anharmonic forces is even smaller.

The pair potential $V(r)$ of Ni found from the data placed on the web site³² using the cubic spline approximation is presented in Fig. 1. In the same figure, the approximation by the fourth-order polynomial using the least-squares method

in the interval $2.496 \pm 0.116 \text{ \AA}$ is also presented. This interval corresponds to the actual values of coordinates of the ILM with the frequency near the top of the phonon band (see Table I). In this approximation, $K_2 \approx 2.32 \text{ eV/\AA}^2$, $K_3 \approx -11 \text{ eV/\AA}^3$, and $K_4 \approx 70 \text{ eV/\AA}^4$. The root-mean-square deviation for the polynomial approximation in the given interval is 10^{-5} eV , i.e., ~ 1000 times less than the corresponding vibrational energy of the bond.

The distance between the nearest atoms in Ni at room temperature is $r_0 = 2.49 \text{ \AA}$ and longitudinal sound velocity is $v_l = 5266 \text{ m/s}$. These values give $\tilde{K}_2 = 2.75 \text{ eV/\AA}^2$ (as expected, $\tilde{K}_2 > K_2$) and $\tilde{\kappa} \approx 1.2$. The distance r_0 increases with temperature ($r_0 = 2.51 \text{ \AA}$ at $T = 800 \text{ K}$) while v_l decreases with temperature ($v_l = 5100 \text{ m/s}$ at $T = 800 \text{ K}$). The $\tilde{\kappa}$ value also decreases with temperature, remaining at $T = 800 \text{ K}$ somewhat larger than 1. Hence, in Ni the condition $\tilde{\kappa} > 1$ is satisfied both at room and at high temperatures.

A fortunate circumstance is that the phonon DOS in Ni (and in other monatomic fcc lattices) has quite a sharp high-frequency peak corresponding to the short-wave phonons (see Fig. 2) resulting in a straightforward localization of the wave packet of these phonons. Consequently, one can expect that in Ni, ILM's can exist with the frequency above the top of the phonon spectrum and that their amplitudes and hence corresponding energies may be relatively small.

To verify this prediction, we performed MD simulations of vibrations of Ni clusters using the full two-body potential without a polynomial approximation. Since the long-range interactions in metals are screened out, the cluster calculations should give reliable results assuming that the size of the cluster is sufficiently large. In our calculations, we studied clusters up to 22 056 atoms with different boundary conditions: (i) periodic, (ii) free ends, and (iii) fixed ends. The results of these calculations agree well with each other. Although the second (volume-dependent) term in Eq. (11) gives only small corrections to forces, it was included in our MD simulations of clusters with periodic boundary conditions.

For the boundary conditions with free and fixed ends, only the linear part of the second term in Eq. (11) was considered. We have found that this approximation does not noticeably change the results but allows one to significantly shorten the calculation time. The resulting phonon-dispersion curves are in satisfactory agreement with those in the literature.³¹

TABLE I. Spatial properties of ILM's in nickel. The difference of the frequency ω_L of the even ILM and the maximum phonon frequency $\omega_M = 5.4 \times 10^{13} \text{ rad/s}$, amplitudes of the bonds \bar{A}_n , and the changes of their length $\bar{\xi}_n$ for the atoms located at $\sqrt{2}r_0[n/2, n/2, 0]$, with $n = 0, 1, 2, 3, 6$, and the resulting ILM energy E . The shifts of atoms of the central chain satisfy the condition $u_{-n} = -u_{n-1}$.

| $\omega_L - \omega_M$ (10^{13} rad/s) | \bar{A}_0 (Å) | \bar{A}_1/\bar{A}_0 | \bar{A}_2/\bar{A}_0 | \bar{A}_3/\bar{A}_0 | \bar{A}_6/\bar{A}_0 | $\bar{\xi}_0$ (Å) | $\bar{\xi}_1/\bar{\xi}_0$ | $\bar{\xi}_2/\bar{\xi}_0$ | $\bar{\xi}_3/\bar{\xi}_0$ | $\bar{\xi}_6/\bar{\xi}_0$ | E (eV) |
|---|-----------------|-----------------------|-----------------------|-----------------------|-----------------------|-------------------|---------------------------|---------------------------|---------------------------|---------------------------|----------|
| 0.013 | 0.116 | 0.853 | 0.534 | 0.267 | 0.050 | 0.007 | 0.571 | -0.143 | -0.286 | -0.0004 | 0.204 |
| 0.081 | 0.142 | 0.845 | 0.514 | 0.239 | 0.023 | 0.008 | 0.750 | -0.250 | -0.375 | -0.0005 | 0.255 |
| 0.181 | 0.180 | 0.844 | 0.522 | 0.250 | 0.034 | 0.014 | 0.571 | -0.143 | -0.357 | -0.0009 | 0.366 |
| 0.465 | 0.314 | 0.863 | 0.564 | 0.287 | 0.022 | 0.034 | 0.618 | -0.059 | -0.235 | -0.003 | 1.080 |
| 0.672 | 0.420 | 0.905 | 0.655 | 0.365 | 0.026 | 0.048 | 0.729 | 0.146 | -0.354 | -0.006 | 2.197 |
| 0.742 | 0.474 | 0.945 | 0.770 | 0.508 | 0.068 | 0.040 | 0.975 | 0.525 | -0.175 | -0.011 | 3.474 |
| 0.779 | 0.500 | 0.966 | 0.852 | 0.640 | 0.094 | 0.030 | 1.100 | 1.000 | 0.267 | -0.016 | 4.596 |

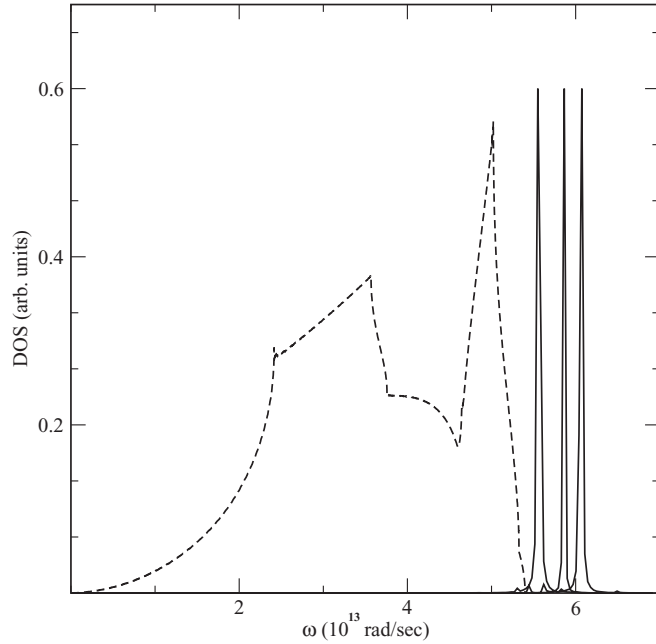


FIG. 2. Phonon density of states and three ILM spectral signatures for Ni. Phonon spectrum (dashed line) and spectrographs (solid line) of the different ILM's: The frequencies are 5.58, 5.86, and 6.07 (10^{13} rad/s) and the amplitudes of vibrations of the central bond are 0.18, 0.31, and 0.42 Å.

Classical molecular dynamics of a Ni cluster was calculated by means of the basic Verlet algorithm:

$$u(t + dt) = u(t) + v(t)dt + \frac{1}{2}a(t)dt^2, \quad (12)$$

$$v(t + dt) = v(t) + \frac{1}{2}[a(t) + a(t + dt)]dt. \quad (13)$$

Here t is time, $u(t)$ is displacement of the atom from its equilibrium position, and $v(t)$ and $a(t)$ are the velocity and acceleration of the atom. The latter were found from Newton's second law by calculating the gradients of E_{tot} with respect to the atom coordinates. For the case of periodic boundary conditions, the periodicity was a cube with edge 52.8 Å, which includes 13 500 atoms. A time step 2 fs was used; 7000 time steps have been calculated, which corresponds approximately to 200 periods of vibrations of the ILM. The results of the calculations are given in Figs. 2 and 3 and in Table I. For the case of free ends, the calculated cluster had 34 parallel $40r_0 \times 17r_0$ square pallets; it includes 23120 atoms. A time step of 0.01 fs was used. A few million time steps were calculated, so that the full calculated time would contain several hundreds of periods of ILM.

In the first runs to excite the lattice vibrations, eight nearest central atoms located at $\sqrt{2}r_0[n/2, n/2, 0], n = -4, -3, \dots, 3$ (in the central chain) have been initially displaced from their equilibrium position constituting an even structure; the displacements u_n of the atoms from their equilibrium position have been chosen as follows: $u_0 = -u_1 = u_2 = -2u_3$. This displacement pattern has the correct symmetry of the ILM but not the exact shape. The values of u_0 varied from 0.09 to 0.3 Å. After the shake off of the phonons at short times, the ILM was recognized as undamped periodic motion at large times (slowly modulated) at a frequency above the maximum of the

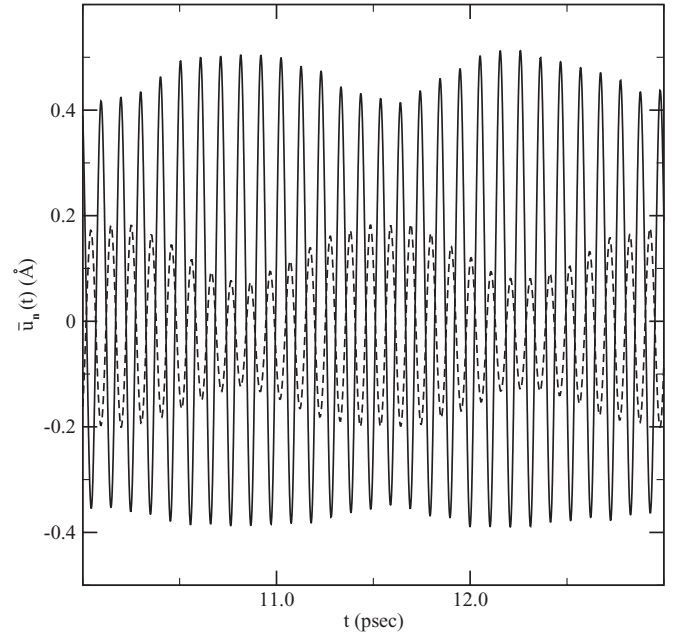


FIG. 3. Time dependence $\bar{u}_n(t) = r_n(t) - r_0$ of the vibration of the central ($n = 0$, solid line) and third ($n = 3$, dashed line) bonds in Ni at long times containing the ILM with the frequency 6.07×10^{13} rad/s. The corresponding values of the dc distortion $\bar{\xi}_n$ are given in Table I. The amplitude modulation of the ILM is induced by its partner, the nearby linear local mode.

phonon band. Figure 3 is an example of the corresponding time dependence of the vibration at long times, where the calculated dependence on time of the difference $\bar{u}_n(t) = r_n(t) - r_0$ for two bonds $n = 0$ and 3 is given.

The dependence of the vibration frequency on the amplitude of the central bonds is presented in Fig. 4; the vibrational amplitudes \bar{A}_n and the dc expansion $\bar{\xi}_n$ of several bonds in the (110) direction are given in Table I. We also calculated several bonds in other directions; the values of corresponding \bar{A}_n and $\bar{\xi}_n$ appeared to be somewhat smaller. As follows from Table I, all seven ILM's presented are quite broad spatially, with the first three essentially keeping the same localization and the other four ILM's broadening. Obviously this is a result of the softening of the pair potential as the amplitude of the ILM's increases. Still, the amplitudes of all such ILM's decrease rapidly in the periphery, as seen from the \bar{A}_6 column.

To control the numerical procedure, the full energy of the cluster was calculated at every time step. The energy conservation law was found to be well fulfilled for the entire calculated time interval. We have also calculated the energy of the ILM; the contribution of 215 atoms situated in a prolate-ellipsoid shape was included in the calculations. It appears that $\sim 2/3$ of the energy of the initially displaced eight central atoms remains localized, while again $2/3$ of it belongs to the atoms in the initially excited chain and $\sim 1/3$ goes to the nearest surrounding atoms. We have found that an ILM in Ni may have a rather small energy ~ 0.2 eV (see the first line in Table I). The reason for this is the existence of the narrow peak in the phonon DOS belonging to short-wave phonons, which permit a rapid splitting of the ILM away from the phonon

band. On the other hand, for large $\bar{A}_0 \geq 0.314 \text{ \AA}$ one observes a significant difference between the ILM frequency and the top phonon frequency; thus we conclude that the existence of ILM's in Ni is reliable.

B. Slow modulation of ILM

Slow modulation of the ILM vibrational amplitude is observed in Fig. 3. The modulation is also seen as a satellite at the frequency $\omega_{LL} = 5.6 \times 10^{13} \text{ rad/s}$ in the spectrum of vibrations of the bonds given in Fig. 5. The weak high-frequency satellite of the triple peak in Fig. 5 results from the nonlinear four-wave mixing $2\omega_L - \omega_{LL}$. This effect has been studied in some detail for a monatomic 1D lattice in Ref. 33 and has been identified with linear local modes (LLM's) associated with the lattice perturbation produced by ILM.

To address the question of whether the modulation observed for this 3D system is connected with artificial size effects or LLM's, we repeated the calculation for a cluster that was twice as large. No significant difference in the time dependence of vibrations of the central atoms was observed. To perform an additional check on our interpretation of the origin of the modulation, a second series of runs has been performed using as the initial conditions the long-time displacement patterns of the 36 atoms (eight atoms in the central chain and seven atoms in every nearest four chains) more closely registered to the correct ILM shape. Now the starting amplitudes of the central particles are determined by averaging over a modulation period. The time dependence of the vibration of the central ($n = 0$) and third ($n = 3$) bonds calculated in this way is presented in Fig. 6. Since the starting shapes more closely resemble a pure ILM eigenvector, the only significant difference from the results shown in Fig. 3 is the reduction of

the amplitude of modulation. The periods of the ILM vibration and of the modulation remain unchanged, precisely what is expected for an LLM of smaller amplitude. This removes the possibility that the observed modulation is associated with the reflection of phonon wave packets from the cluster boundary.

This conclusion also agrees with our calculation of vibrations of atoms near the border. The amplitudes of these border vibrations always remain less than or of the order of $5 \times 10^{-3} \text{ \AA}$, i.e., they are much smaller than the amplitude of modulation of vibrations of the central atoms.

All of these signatures allow us to assign the observed modulation to the linear local mode produced by the ILM. Indeed, as expected for a LLM, its frequency increases with increasing amplitude and frequency of the ILM. An enlargement of the modulation for the side bonds shows, in agreement with Ref. 33, that the maximum amplitude of the LLM is situated in the periphery of the ILM. An interesting property of the mode, which causes the modulation, is the change of the sign of the frequency difference $\omega_L - \omega_{LL}$ with decreasing localization of the ILM. For the ILM in the first line of Table I, $\omega_L - \omega_{LL}$ is negative ($-0.14 \times 10^{13} \text{ rad/s}$), while for ILM's in all other lines it is positive (0.17, 0.24, 0.42, 0.45, 0.38, and 0.35, respectively, all in 10^{13} rad/s units). This change of sign is also expected for the LLM: it results from the different dependence of the ILM and LLM on the even anharmonicities.³³

In order to verify the conclusion about the existence of ILM's in Ni at elevated temperatures, we repeated the calculations presented in Fig. 6 for the lattice constant corresponding to 800 K. We found that the ILM also exists at this temperature but with slightly enlarged ($\sim 3\%$) amplitude and reduced frequency $\omega_L = 5.67 \times 10^{13} \text{ rad/s}$. Thermal fluctuations characteristic of nonzero temperature in the initial

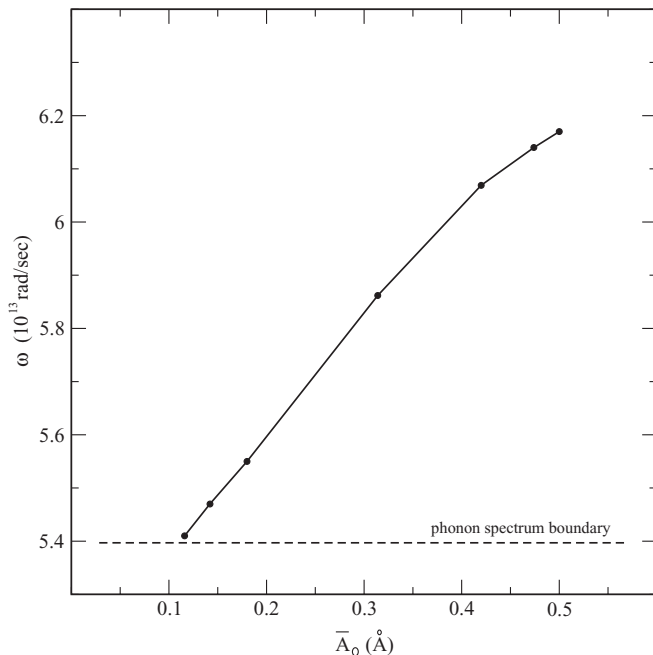


FIG. 4. The dependence of frequency ω_L of the even ILM in Ni on the amplitude of vibrations of the central bond.

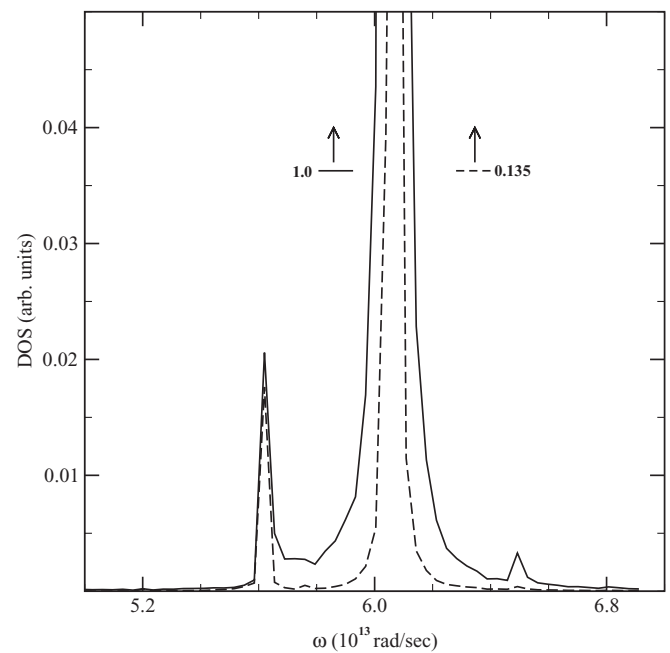


FIG. 5. ILM with its satellite LLM ($\omega_L = 6.07 \times 10^{13} \text{ rad/s}$). Shown are the Fourier transforms of vibrations $\bar{u}_0(t)$ (solid line) and $\bar{u}_3(t)$ (dashed line) given in Fig. 3.

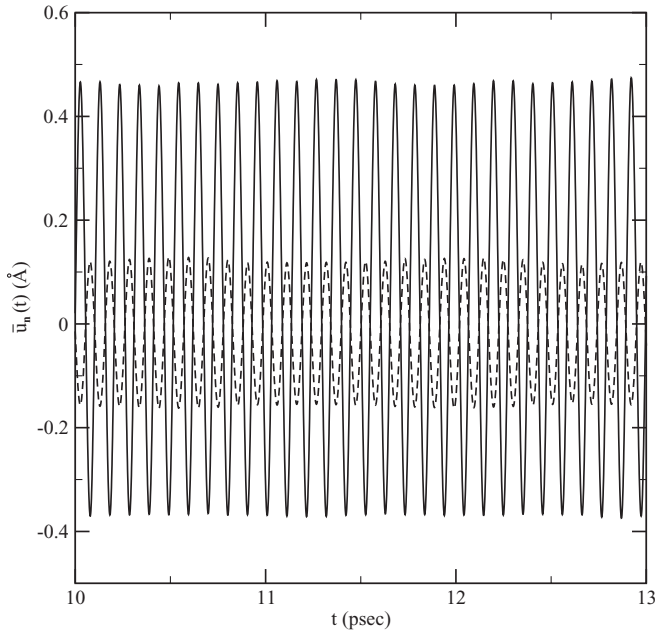


FIG. 6. The same time dependence $\bar{u}_n(t) = r_n(t) - r_0$ of the vibration of the central ($n = 0$, solid line) and third ($n = 3$, dashed line) bonds in Ni at long times, as shown in Fig. 3. The initial shifts of the 36 central atoms (eight atoms in the central chain and seven atoms in every nearest four chains) are more closely described by the correct ILM shape. The starting values of the shifts are obtained by averaging over a modulation period in Fig. 3. Since the ILM shape is more closely approximated, the modulation amplitude is greatly reduced as compared to Fig. 3.

state have been ignored; however, thermal-like fluctuations appeared in our MD simulations in the latter stages of the time evolution of the system due to shaking-off of the phonons. These fluctuations do not significantly affect the ILM.

C. ILM's in niobium

In contrast with nickel, niobium is isotopically pure and may provide a cleaner experimental signature for the observation of intrinsic localization. Using an analogous algorithm, we also performed molecular-dynamics simulations of ILM's in Nb. The peculiarity of this metal is the rather slow screening of the interactions with increasing distance between the ions. For a correct description of the phonon DOS, one needs to take into account the elastic forces between at least six nearest-neighboring atoms.³⁴

The existing EAM theories of Nb do not describe sufficiently well the atomic forces for such a large spatial interval. Therefore, we did not use them in a description of the linear dynamics. Instead, for this purpose the force constants for six nearest neighbors given in Ref. 34 were used. Thus, for Nb we did not use the single pair potential for MD simulations (as we did for Ni). Instead, we used six different potentials (more precisely, we used six different forces) for every six nearest atom pairs.

The EAM potential of Ref. 35 was used only to find the anharmonic forces, namely, the three nonlinear forces for the three nearest atoms. Corresponding to this EAM,

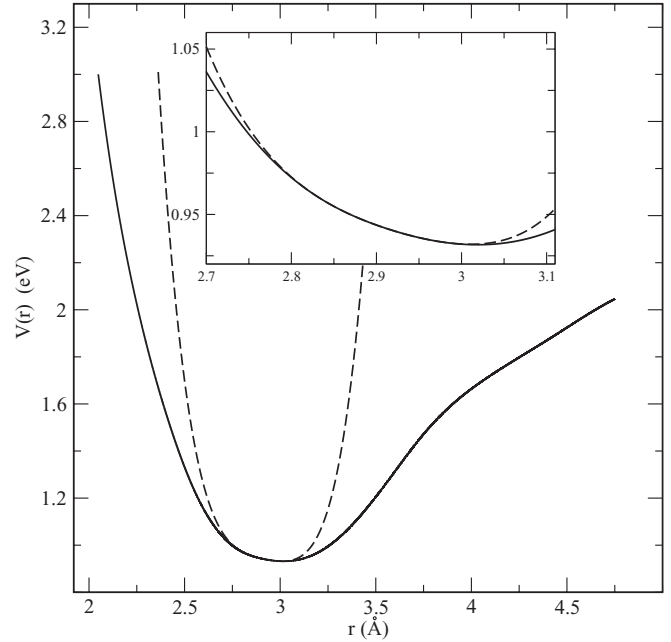


FIG. 7. The pair potential $V(r)$ of Nb (solid line) and its approximation by the fourth-order polynomial (dashed line). The inset shows an expanded view.

the pair potential $V(r)$ as well as its approximation by the fourth-order polynomial are presented in Fig. 7 (corresponding parameters are $K_2 \approx 1.5 \text{ eV}/\text{Å}^2$, $K_3 \approx -6.2 \text{ eV}/\text{Å}^3$, and $K_4 \approx 65.6 \text{ eV}/\text{Å}^4$; the root-mean-square deviation for the polynomial approximation in the interval between 2.82 and 2.97 Å is 10^{-5} eV). This $V(r)$ is equal to the first term of the EAM given by Eq. (3) in Ref. 35 plus the linear part at r_0 of the second term in this equation (r_0 is the equilibrium distance of the nearest atoms at given temperature). The anharmonic forces were found as follows: for each of the three nearest atom pairs, we deleted from the potential given in Fig. 7 the linear and quadratic terms at equilibrium distance. Then we added to each of these nonlinear forces the corresponding linear force given by Ref. 34.

The same source was used to obtain the remaining three linear forces between the atom pairs at larger distances. The justification for this approximation is that the relative change in distance of the fourth, fifth, and sixth atom pairs for the ILM's with the maximum amplitude $\sim 0.1 \text{ Å}$ is a few percent. For such small relative shifts and large distances, the anharmonic forces are negligibly small. Therefore, for a description of ILM's with small amplitude, one may use the known elastic forces for six nearest neighbors³⁴ and take into account the anharmonic forces only for three nearest neighbors.

Using the algorithm described above, we performed MD simulations of ILM's in Nb for room temperature 293 K (equilibrium first neighbor distance $r_0 = 2.86 \text{ Å}$, longitudinal velocity of sound $v_l = 5380 \text{ m/s}$) and high temperature 1773 K ($r_0 = 2.89 \text{ Å}$, $v_l = 5073 \text{ m/s}$). For both temperatures, $\bar{\kappa} > 1$, i.e., the derived condition of an ILM with frequency above the phonon spectrum is fulfilled. The calculations at room temperature were done for a cluster containing $2 \times 40 \times 40 \times 40$

moving atoms (altogether 128 000 atoms). The calculations at high temperature were done for a cluster elongated in the [111] direction with C_{3h} symmetry (a hexagonal prism) containing 18 760 moving atoms. To minimize the calculation time, the positions and velocities of 1/6 of the atoms, situated in one of the six identical segments of the prism, were calculated at every time step; the positions and velocities of all other atoms were found from the symmetry conditions.

For both sets of lattice parameters, we have found even ILM's in the [111] direction of vibrations of the central atoms with frequencies above the top of the phonon spectrum. These ILM's are fully stable: no decay of their amplitude was observed over the last 500 periods of vibrations. A small periodic modulation of the amplitude, analogous to Ni, was also observed, presumably caused by the appearance of a linear local mode. The spectra of ILM's for two different amplitudes of vibrations of the central bond are presented in Figs. 8 and 9 (together with the phonon spectrum). As expected, the frequency of the ILM increases with amplitude.

To check the specificity of the above procedure, we also performed calculations of ILM's in Nb taking into account the full potential given in Ref. 35 [including the volume-dependent second term in Eq. (10)]. At high temperatures, stable ILM's do exist for this model. In addition, we found that the formation of ILM's in Nb is favored by the expansion of the Nb lattice with increasing temperature.

On the other hand, based on the relations presented here, we have found that at least in some other metals (e.g., in Al and Cu), ILM's of the type described here should not exist. Indeed, the values of the parameter $\tilde{\kappa}$ in these metals at room temperature are found to be 0.3 (Al) and 0.38 (Cu) (using

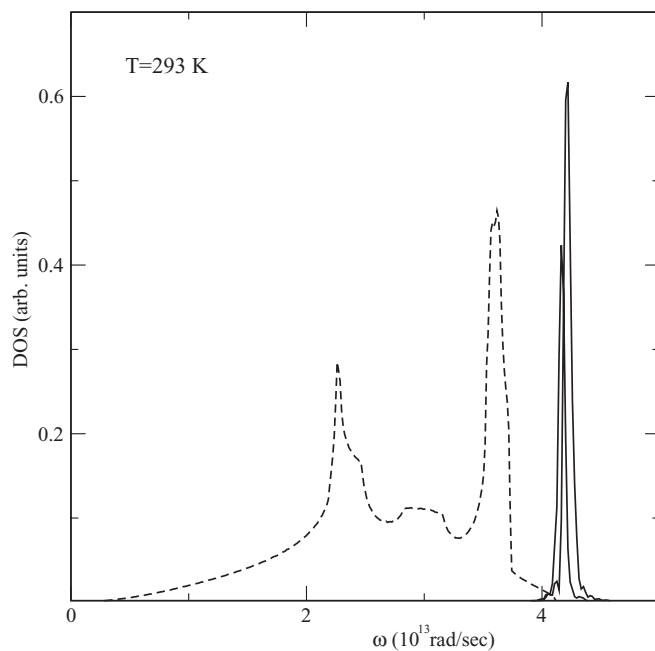


FIG. 8. Phonon DOS and spectra of even ILM's in Nb at room temperature 293 K for two amplitudes (0.25 and 0.3 Å) of vibrations of the central bond. Solid lines: ILM's, dashed line: phonon spectrum of Nb.

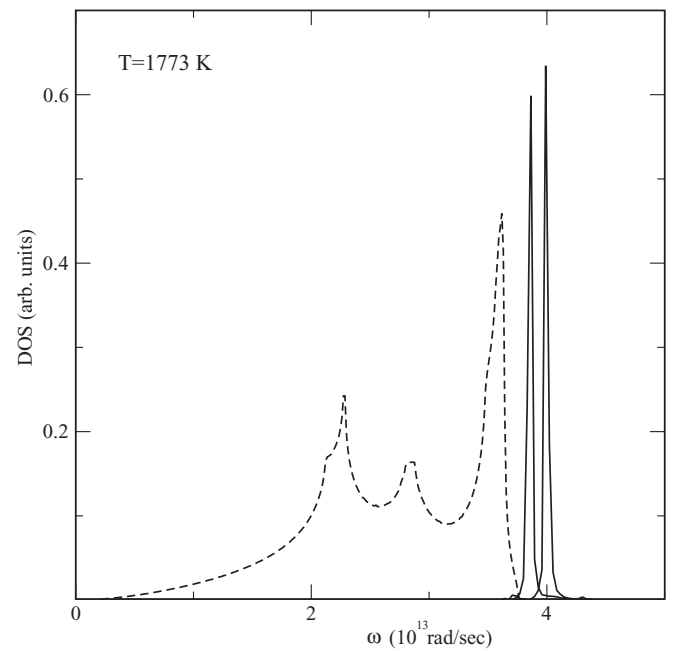


FIG. 9. Phonon DOS and spectra of even ILM's in Nb at a high temperature (1773 K) for two amplitudes (0.085 and 0.12 Å) of vibrations of the central bond. Solid lines: ILM's, dashed line: phonon spectrum of Nb.

the potentials given in Ref. 32). At 800 K, these parameters are equal to 0.1 and 0.42, respectively. All these values are much smaller than the border value 1, which makes it unlikely that ILM's of the type described here can appear in these metals.

IV. CONCLUSION

To sum up, we performed an analytic and numerical study of nonlinear dynamics of Ni and Nb, and we found that intrinsic localized modes may exist in these metals with frequencies above the top of the phonon bands. The physical reason for this is the relatively large value of even anharmonicities as compared to odd ones produced by the free electron screening of the atomic interactions. As a result, in Ni and Nb (and presumably in some other metals), the ion-ion attractive force at intermediate distances is enhanced, resulting in the amplification of even anharmonicities for the two-body potentials. This effect counteracts the underlying softening associated with the bare potentials with a moderate increase of vibrational amplitudes to permit the existence of ILM's above the top of the phonon spectrum. In our MD simulations of nonlinear dynamics of Ni and Nb, we have clearly observed ILM of this type. In addition, we also observed the linear local modes associated with an ILM; modes of this type have been predicted recently and observed numerically for chains in Ref. 33. According to our calculations, an intrinsic localized mode in Ni or in Nb may have a rather small amplitude and hence a small energy of formation. We expect that in these metals, ILM's may be observed as high-frequency features in the phonon spectrum at high temperatures. Finally, we note that the precision of the

existing EAM models of Nb is rather low;^{35,36} however, the EAM models of Ni are usually considered to be quite precise.³¹ Therefore, the conclusions presented here about ILM's in Ni are expected to be more reliable than those about ILM's in Nb.

ACKNOWLEDGMENTS

The research was supported by ETF Grants No. 7741 and No. 7906 and by the European Union through the European Regional Development Fund (project TK114). A.J.S. was supported by NSF-DMR-0906491.

-
- ¹B. R. Henry, *J. Phys. Chem.* **80**, 2160 (1976).
²M. L. Sage and J. Jortner, *Adv. Chem. Phys.* **47**, 293 (1981).
³A. A. Ovchinnikov and N. S. Erihman, *Sov. Phys. Usp.* **25**, 738 (1982).
⁴B. R. Henry and H. G. Kjaergaard, *Can. J. Chem.* **80**, 1635 (2002).
⁵A. M. Kosevich and A. S. Kovalev, *Zh. Eksp. Teor. Fiz.* **67**, 1793 (1974) [*Sov. JETP* **40**, 891 (1974)].
⁶A. S. Dolgov, *Fiz. Tverd. Tela (Leningrad)* **28**, 1641 (1986) [*Sov. Phys. Solid State* **28**, 907 (1986)].
⁷A. J. Sievers and S. Takeno, *Phys. Rev. Lett.* **61**, 970 (1988).
⁸J. B. Page, *Phys. Rev. B* **41**, 7835 (1990).
⁹R. S. MacKay and S. Aubry, *Nonlinearity* **7**, 1623 (1994).
¹⁰S. A. Kiselev and V. I. Rupasov, *Phys. Lett. A* **148**, 355 (1990).
¹¹S. R. Bickham, A. J. Sievers, and S. Takeno, *Phys. Rev. B* **45**, 10344 (1992).
¹²K. W. Sandusky, J. B. Page, and K. E. Schmidt, *Phys. Rev. B* **46**, 6161 (1992).
¹³A. J. Sievers and J. B. Page, in *Dynamical Properties of Solids: Phonon Physics. The Cutting Edge*, edited by G. K. Norton and A. A. Maradudin (North Holland, Amsterdam, 1995), Vol. VII, p. 137.
¹⁴S. Flach and C. R. Willis, *Phys. Rep.* **295**, 182 (1998).
¹⁵R. Lai and A. J. Sievers, *Phys. Rep.* **314**, 147 (1999).
¹⁶D. K. Campbell, S. Flach, and Y. S. Kivshar, *Phys. Today* **57**(1), 43 (2004).
¹⁷M. Sato, B. E. Hubbard, and A. J. Sievers, *Rev. Mod. Phys.* **78**, 137 (2006).
¹⁸S. Flach and A. Gorbach, *Phys. Rep.* **467**, 1 (2008).
¹⁹S. A. Kiselev, S. R. Bickham, and A. J. Sievers, *Phys. Rev. B* **48**, 13508 (1993).
²⁰S. A. Kiselev and A. J. Sievers, *Phys. Rev. B* **55**, 5755 (1997).
²¹V. Hizhnyakov, D. Nevedrov, and A. J. Sievers, *Physics B* **316–317**, 132 (2002).
²²L. Z. Khadeeva and S. V. Dmitriev, *Phys. Rev. B* **81**, 214306 (2010).
²³M. E. Manley, M. Yethiraj, H. Sinn, H. M. Volz, A. Alatas, J. C. Lashley, W. L. Hulst, G. H. Lander, and J. L. Smith, *Phys. Rev. Lett.* **96**, 125501 (2006).
²⁴M. S. Daw and M. I. Baskes, *Phys. Rev. B* **29**, 6443 (1984).
²⁵M. S. Daw and M. I. Baskes, *Phys. Rev. Lett.* **50**, 1285 (1983).
²⁶W. A. Harrison, *Solid State Theory* (McGraw Hill, New York, 1970).
²⁷V. Hizhnyakov, A. Shelkan, and M. Klopov, *Phys. Lett. A* **357**, 393 (2006).
²⁸A. Shelkan, V. Hizhnyakov, and M. Klopov, *Phys. Rev. B* **75**, 134304 (2007).
²⁹B. Sanchez-Rey, G. James, J. Cuevas, and J. F. R. Archilla, *Phys. Rev. B* **70**, 014301 (2004).
³⁰S. R. Bickham, S. A. Kiselev, and A. J. Sievers, *Phys. Rev. B* **47**, 14206 (1993).
³¹Y. Mishin, D. Farkas, M. J. Mehl, and D. A. Papaconstantopoulos, *Phys. Rev. B* **59**, 3393 (1999).
³²[<http://cst-www.nrl.navy.mil/bind/eam>].
³³V. Hizhnyakov, A. Shelkan, M. Klopov, S. A. Kiselev, and A. J. Sievers, *Phys. Rev. B* **73**, 224302 (2006).
³⁴F. Guthoff, B. Hennion, C. Herzig, W. Petry, H. R. Schober, and J. Trampenau, *J. Phys. Condens. Matter* **6**, 6211 (1994).
³⁵M. R. Fellinger, H. Park, and J. W. Wilkins, *Phys. Rev. B* **81**, 144119 (2010).
³⁶A. M. Guellil and J. B. Adams, *J. Mater. Res.* **7**, 639 (1992).